

GLD1023

10/1/78  
3-11-1980

SEISMIC EMISSIONS STUDY

BEOVAWE, NEVADA

Prepared for:

Chevron Resources Company

Jan 1978

By:

Lewis Katz  
Seismic Exploration Inc.  
Salt Lake City, Utah

## TABLE OF CONTENTS

	Page
List of Illustrations and Enclosures . . . . .	i
Introduction . . . . .	1
Background . . . . .	1
Data Acquisition . . . . .	2
Data Processing . . . . .	2
Data Analysis . . . . .	3
Data Interpretation . . . . .	4
Conclusions . . . . .	5
Appendix A. Data Format . . . . .	A-1

## List of Illustrations and Enclosures

### Computer Plots and Printouts for:

Station 1,  
Station 3,  
Station 4,  
Station 5.  
Composite

### Contour Maps:

1. Contour Map Top of Seismic Emissions Anomaly Station: 1
2. Contour Map Top of Seismic Emissions Anomaly Station: 3
3. Contour Map Top of Seismic Emissions Anomaly Station: 4
4. Contour Map Top of Seismic Emissions Anomaly Station: 5
5. Composite Map Top of Seismic Emissions Anomaly

## SEISMIC EMISSIONS STUDY

### BEOWAVE, NEVADA

#### Introduction

At the request of Chevron Resources Company, a Seismic Emissions Study was performed at Beowawe, Nevada (Whirlwind Valley, Lander and Eureka Co's.) The areal extent of this survey was approximately 16 square miles. Five 5 geophone arrays were used to collect seismic emission data over this region for the purpose of delineating active fault and fracture zones possibly associated with magmatic activity.

#### Background

Whirlwind Valley (Beowawe) is located in the Basin and Range physiographic province. Local surface topography is characterized by what appears to be a normal fault (Malpais) of about 600 ft. throw striking northeast. Whirlwind Valley lies downthrown to the northwest of the fault and the Malpais Range on the upthrown block toward the southeast. Several geysers and hot springs can be seen on the downthrown block apparently associated with the fault. Figure 1, shows a geological map of the area (Stewart and Carlson, 1976-Geological Map of North-Central Nevada). Faults are shown at the geysers and in the southwest quarter of the survey area. Several inferred faults (dotted) are shown striking parallel but basin inward to the observed Malpais fault. Geothermal exploration targets are often localized over fault and fracture zones since they form conduits and reservoirs for hot fluids. One method of locating these geothermal zones is to utilize a seismic emission study.

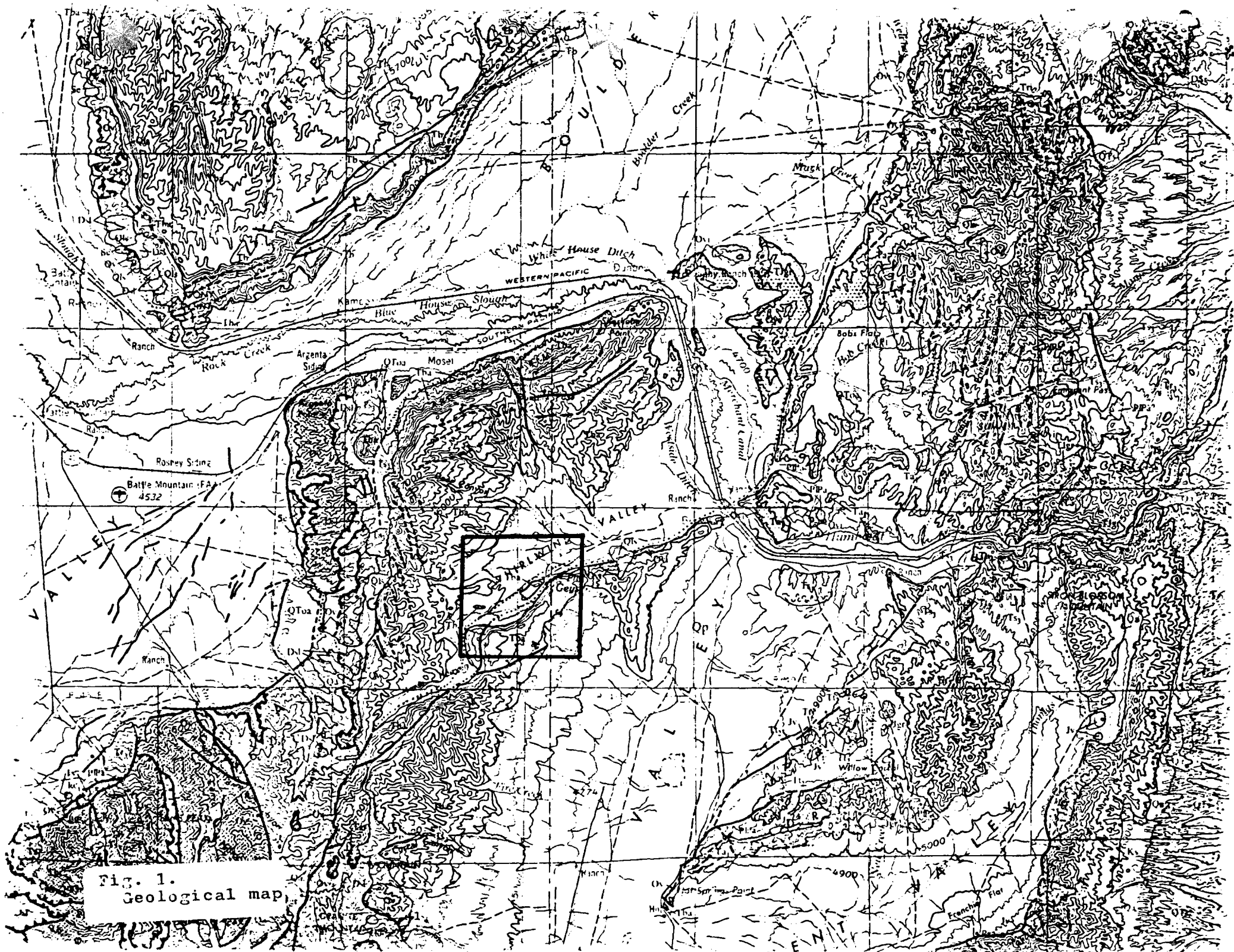


Fig. 1.  
Geological map

### Data Acquisition

Five Sprengnether MEQ-800 microearthquake recording systems, together with Datamagnetics digital tape recorders, were used for field data acquisition. Hall Sears HS-1 (1 Hz) geophones with calibration coils were used as sensors. The digital tape recorders feature high dynamic range and low system noise recording. The MEQ-800 offers smoked paper records for field monitoring of the data. Geophones were spaced approximately 2000 feet apart. Individual recording systems were hard wired together so that absolute relative timing could be obtained by broadcasting time marks every hour. The crystal clocks supplied by the manufacturer in the MEQ-800's are temperature dependent causing drifts greater than 20 msec. These drifts are not linear and therefore cannot be scaled by a correction factor. Stations were occupied from one to two days, depending on the quality of data observed on the paper records.

### Data Processing

Field data were first edited by picking quiet sections from the smoked paper records. These sections were stripped out and re-edited. Data from four stations (1,3,4,5) were chosen for processing. For each station, four depth arrays (20 x 20) of possible source locations were chosen at 1,050 foot intervals. That is, four 19,950 x 19,950 foot horizontal maps were generated at depths of 2000, 4000, 6000, and 8000 feet. Ray tracing algorithms were used to determine delay times from each source location to the geophones at each station. Geophone arrays were focused on each location by shifting traces by appropriate delay times and then stochastically correlating traces. Five hours of array processing time per station was required (6800

correlations). A listing of individual delay times, correlation values, and graphic plots were produced.

### Data Analysis

Data were processed using two velocity models, a half-space model of 16,000 fps and a layered model varying from 6,000 fps at the surface to 16,000 fps from 2,900 ft. and below. Both models appear to give the same results with no apparent differences in location of groundnoise sources. Also, two sets of independent data were processed in order to verify initial results and stationarity of source locations. With the exception of station 5 all data were reproducible. Composite computer plots were created by averaging results from all stations.

On the computer plots, the higher the intensity of shading the higher the correlation values. Caution must be taken when interpreting computer plots. These plots were created as a visual aid by scaling correlation values between zero and ten for each station set. The maximum correlation value was scaled to ten. Therefore, plot intensities may represent different values at different stations and it is possible that a high correlation value could distort the entire plot.

Maps showing locations of correlation values greater than 50% and 90% of maximum have been made for stations 1, 3, 4, and 5. These should be examined in conjunction with computer plots to reduce the possibility of misinterpretation. That is, by examining these together, lateral extent and thickness of anomalies will be more obvious. Smearing (fanning) or blurring of the anomalies can be seen as you focus on points further away from the station. This may be caused by two factors. First, as you go further away from the array, differences in travel times between geophones

decrease (become similar). Secondly, higher frequencies attenuate with distance and the correlation is performed over a narrower frequency band.

In most cases points seen on the plots are not resolved uniquely because several points may have the same or similar differences in delay times. Therefore, a vector is seen pointing toward or through the noise source. By using the intersection of vectors from several stations the anomalous region is defined uniquely.

### Data Interpretation

The purpose of this survey was to map locations of seismic emissions (groundnoise) as a means of delineating zones of permeability (faults and fractures). Inferred faults (dashes and dots) and associated fracture zones (solid or dashed lines) mapped using seismic emissions are shown on the composite map enclosed. Multi-layered velocity models were used at Stations 1 and 3 (downthrown block) and a half-space model of 16,000 fps at Stations 4 and 5 (upthrown).

Three anomalous zones are identified. Anomaly A is rated the highest since vectors from all stations intersect at this point. Although Station 1 is influenced more by Anomaly B, on the computer plots some activity is shown coming from the direction of Anomaly A. Anomaly B is formed from the intersection of vectors from stations 5 and 1. Maximum correlation values from each station appear at this location. However, it may be possible to move vector 1 slightly to the north which would result in the anomalous region appearing approximately at Station 4. Therefore, vectors from Stations 1, 4, and 5 would intersect over Station 4. Station 3 being further away from this region does not appear to be influenced by it. Anomaly C was determined from results at Stations 3 and 5. Station 1 also sees activity



from this area and Station 4 appears to be too far away.

Inferred faults are shown on the composite map. These actually reflect the locations of high correlation values as seen on the computer plots. However, these locations are not defined uniquely since points lying along these vector directions have the same or similar differences in delay times. This is why the intersection of vectors is used to uniquely determine the anomalous regions.

From Figure 1, a mapped fault can be seen going through the center of Anomaly C. This fault is also reflected in the topography since it corresponds to a gorge or steep valley-like structure. Using the same criteria the inferred faults through Anomaly B and Station 4 can be seen corresponding to topographic lows and steep valleys or gorges. The inferred fault through Station 4 crosses through a group of hot springs and the steep gorge located just below this Station. The northwest strike of these faults is consistent with the direction of regional strike seen on the northwest side of Whirlwind Valley (Figure 1).

On the composite computer plot a central region of no correlation can be seen. This corresponds to the observed Malpais fault being locked-in at this location. That is, no seismic emissions (noise) are being emitted from the central region of the fault.

### Conclusions

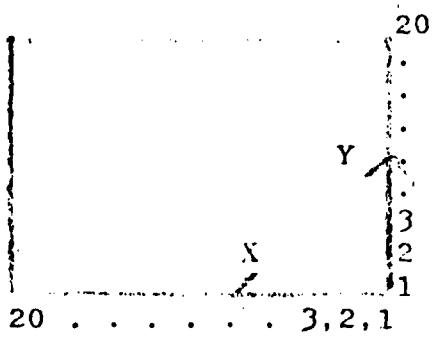
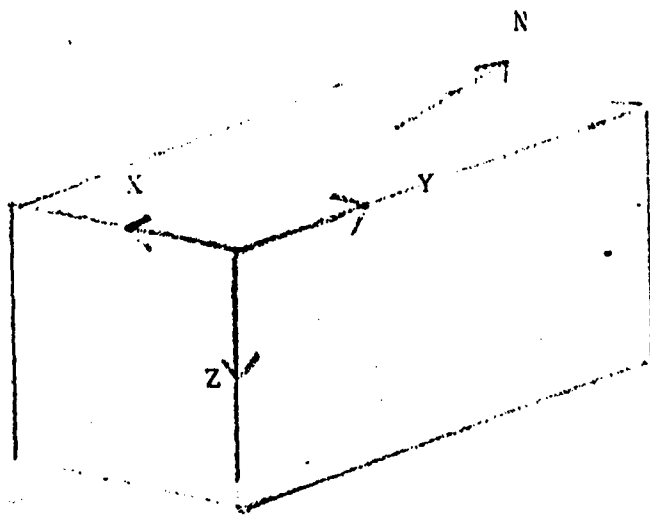
Evidence of groundnoise being emitted from three locations within the survey area has been determined. Although inferred faults through these regions have been assumed, the technique used here is not capable of delineating their existence outside the anomalous regions. The Malpais fault appears to be locked-in at the center section of the survey and is a more

active noise generator toward the ends. This suggests that the migration of fluids or an active fracture system is more likely associated with the end sections of the fault where the anomalous regions (B & C) occur. It is possible that Anomaly B can be moved closer to Station 4. An anomalous region (A) located in the northwest portion of the survey indicates this location is worthy of further investigation.

## APPENDIX A

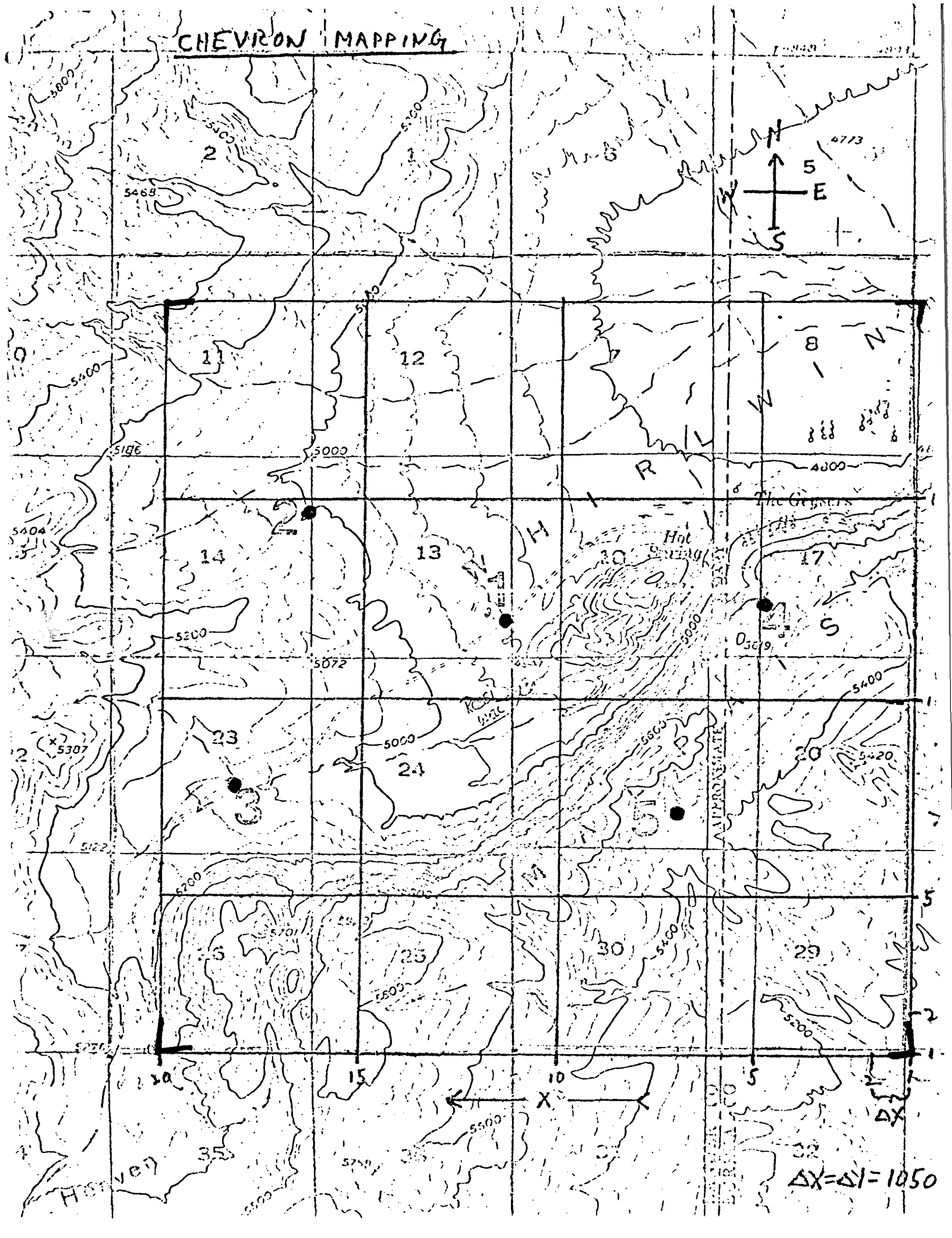
### Data Format

X-Y computer plots are read from the lower right hand corner (east) as point (1,1,1) [X,Y,Z]. Going from right to left across the bottom points are (1,1,1), (2,1,1), (3,1,1). . . . Similarly, the second horizontal row is labeled from right to left (1,2,1), (2,2,1), (3,2,1). . . . The center Y value indicates the horizontal row and the end Z value the depth. Each iteration is 1050 feet except for the Z values which are 2000 feet. Z values 1, 2, 3, and 4 correspond to depths of 2000, 4000, 6000, 8000 feet, respectively.



Numbering is east to west and surface downward.

# CHEVRON MAPPING



:OT 10:53:52 } 4' 33"  
 11/14/77 10:49:19 }  
 :IO, 9, 17 }  
 :QUB, CONDIO/ISR }  
 0 1 0

11/14/77

Braumen  
 ESS1205 (Time 4' 33")

(COMBIO/ISSPID) on CH 1-NESW (PK-28)

INPUT: LUNA(AT) BARC-1F41 (Point of FOL 30 [Point] on  
 CH 1-NESW F2P.T.S., PK-28 (T 0741-54), Mode 1,  
 VE=1.0, 11/10 11/02/77-1 (CNML), XY 1-4 (2000',  
 4000', 6000', 8000'), 20 x 20 Grid

(ISSPID) BARC-1 F41 (Time)

Copy 2 of 2  


---

 CHEVRON 1 - N, E, S, W (PK-28)

FOCUS (Product Version, Correlation Function reversed if negative) on  
 Filtered T.S., Prices 15-28 (Times 0741-0754), Mode 1,  
 CHEVRON Multi-Layer Vel. Prof. (see below),  
 XY slices 1-4 (2000', 4000', 6000', 8000'), 20 x 20 Grid

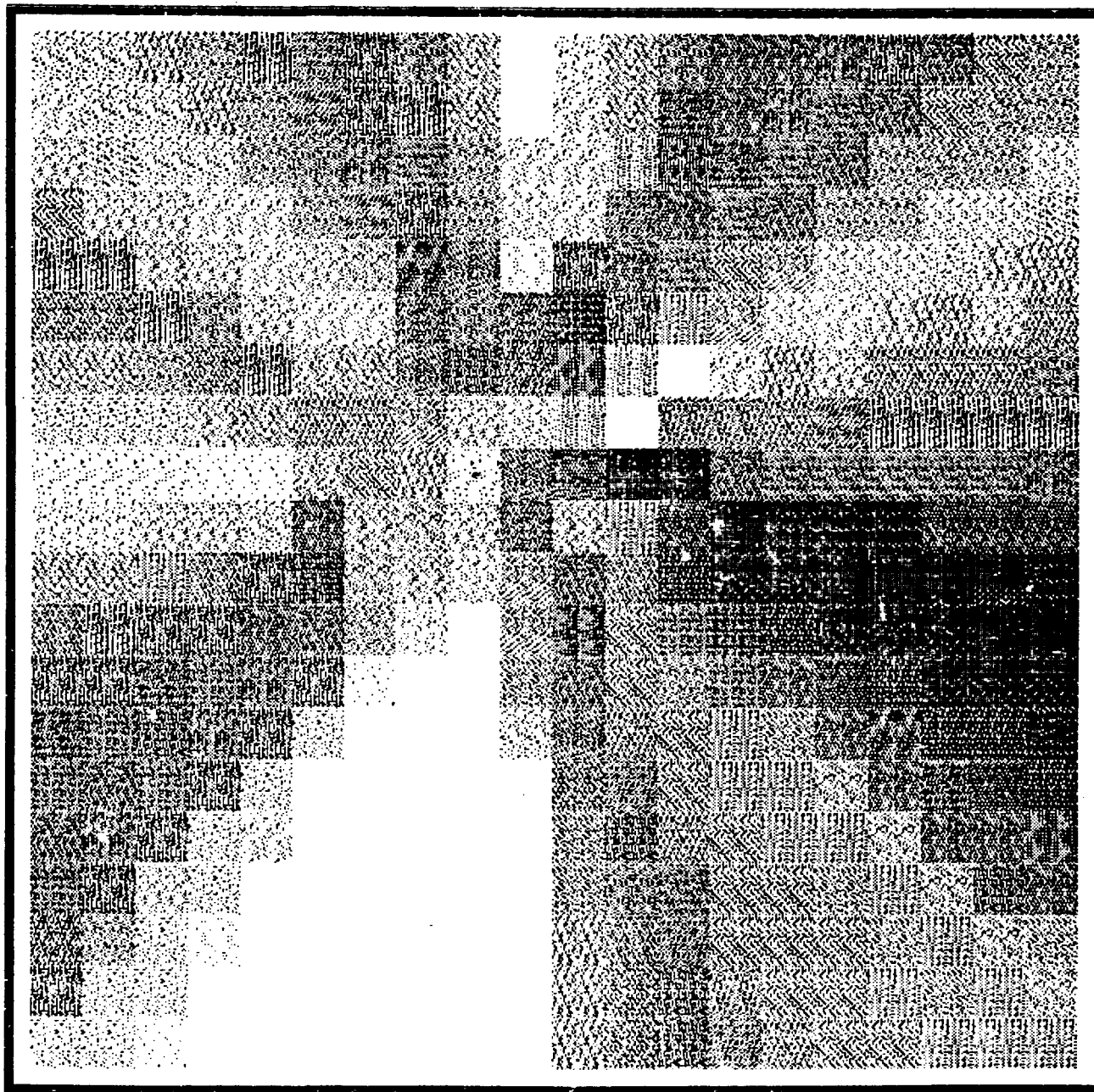
---

 Slowness Plot of Same

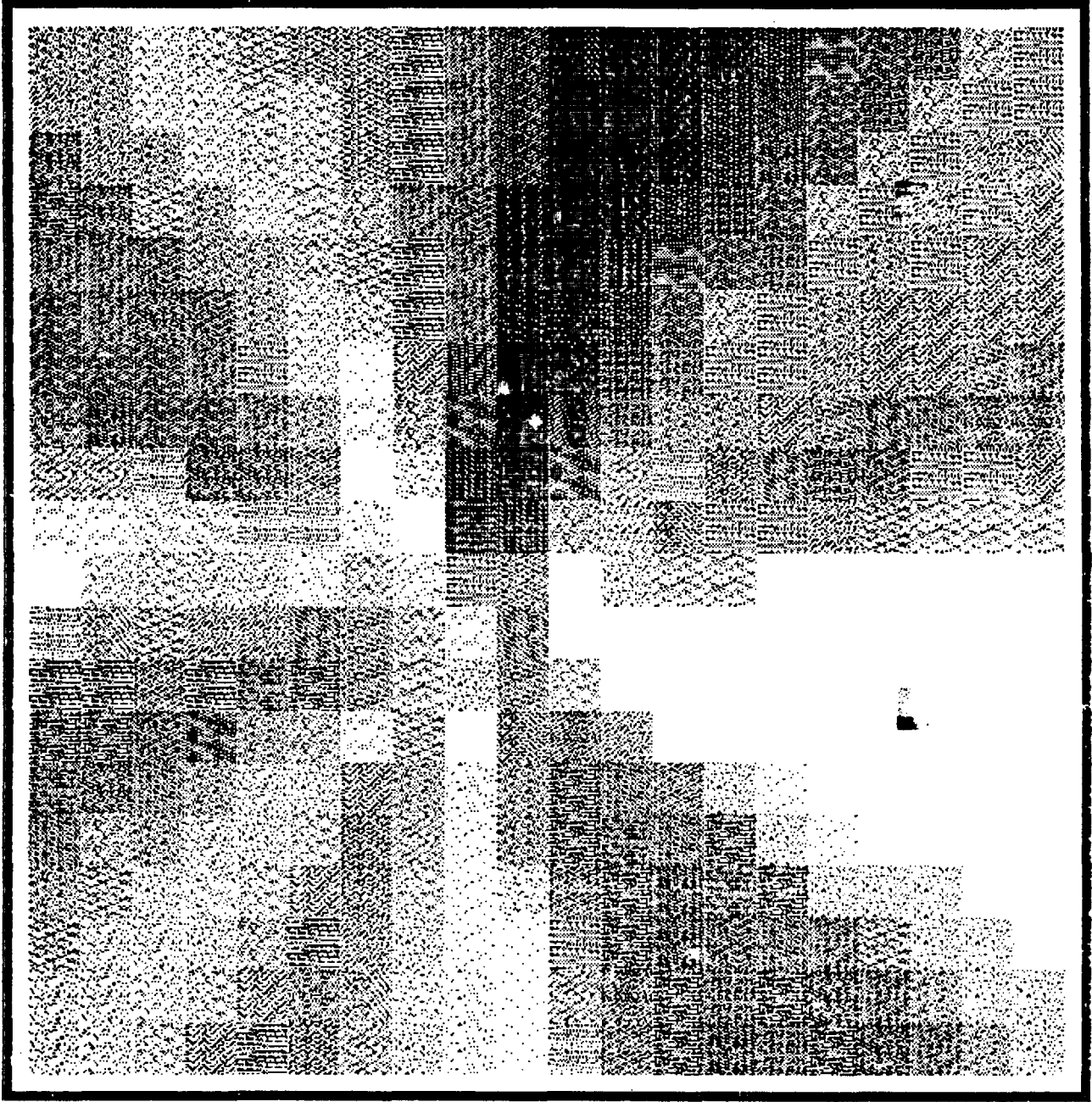
Vel. Prof.

Layer #	Vel (ft/sec)	Layer (ft)
1	6000	
2	7000	1000
3	8500	1500
4	11500	2000
5	12500	2200
6	13500	2500
7	14000	2700
8	16000	2900

Station 1

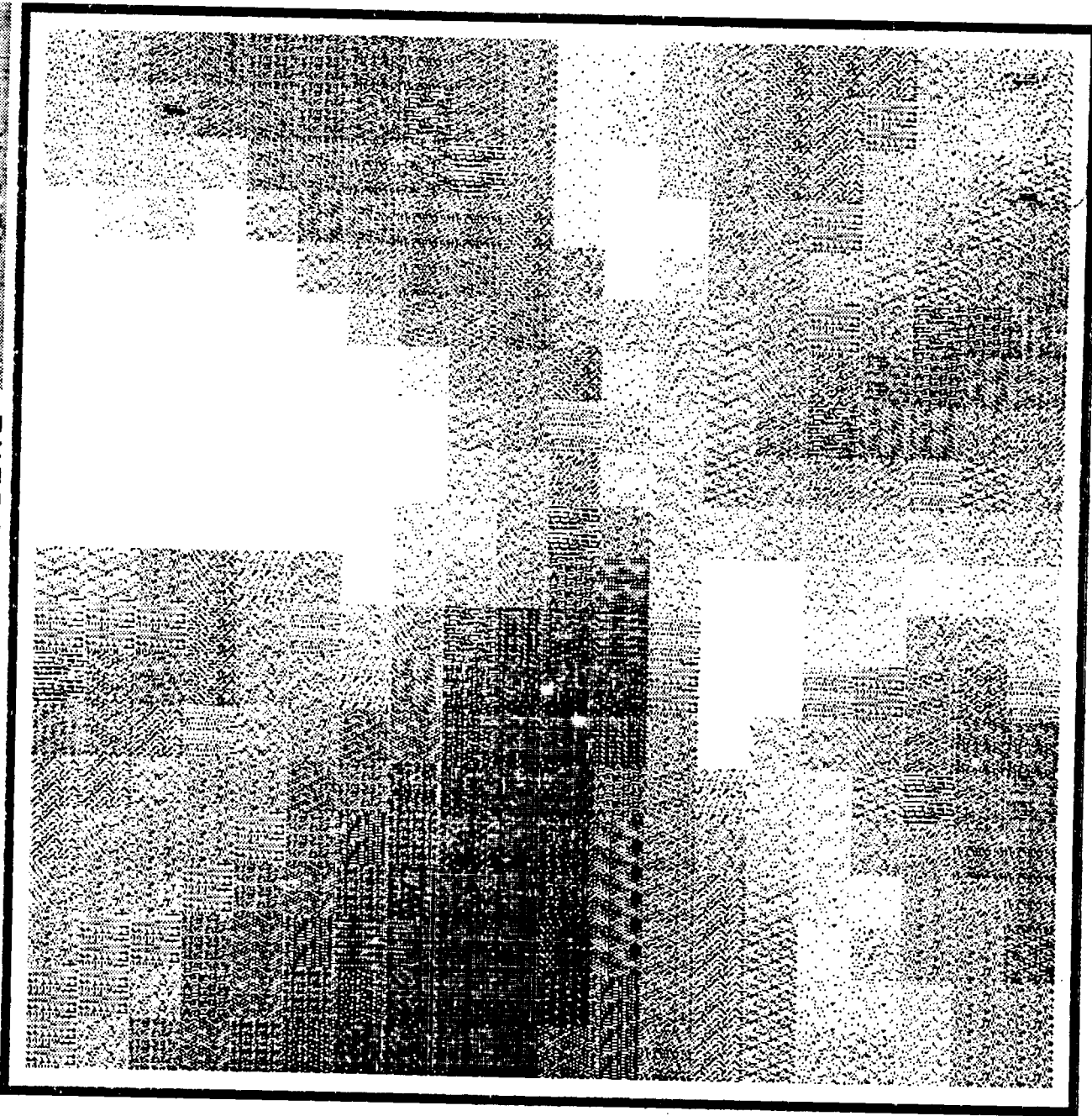


XY PLOT SLICE 2

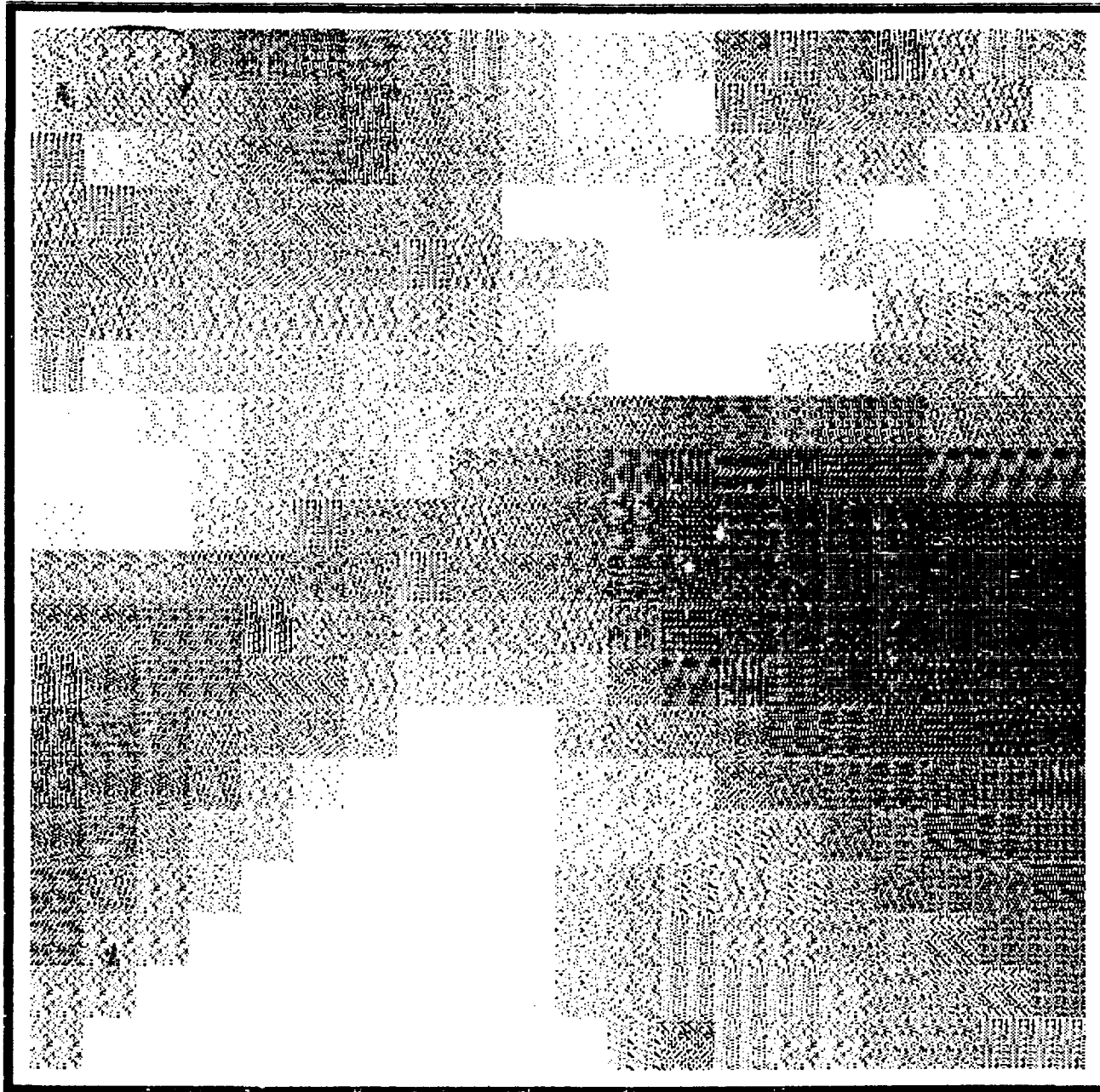


ENSCO, INC.





ENSCO, INC.



OT 10:58:28 } 4'33"  
 11/14/77 10:53:55 }  
 IO, 9, 17 }  
 QUB, CONDIO/ISR }  
 0 1 0

9/14/77

Bairman  
 ESS 1205 (Time 4'33")

DISP3D on CH3B-CNE (PIS-27)  
 INPUT LUN4 (T1) RARC-1F43 (Print of FOCUS (PIS-27)  
 on CH3B-CNE Filt. T.S., PIS-27 (TOM-37),  
 Mode 1, VF=1.0, HYPO 1/12/77 (CHML), XY 4  
 (2000', 4000', 6000', 8000'), 20 \* 20 Grid  
 (DISP3D RARC-1F44 (Trans))

Copy 2 of 2

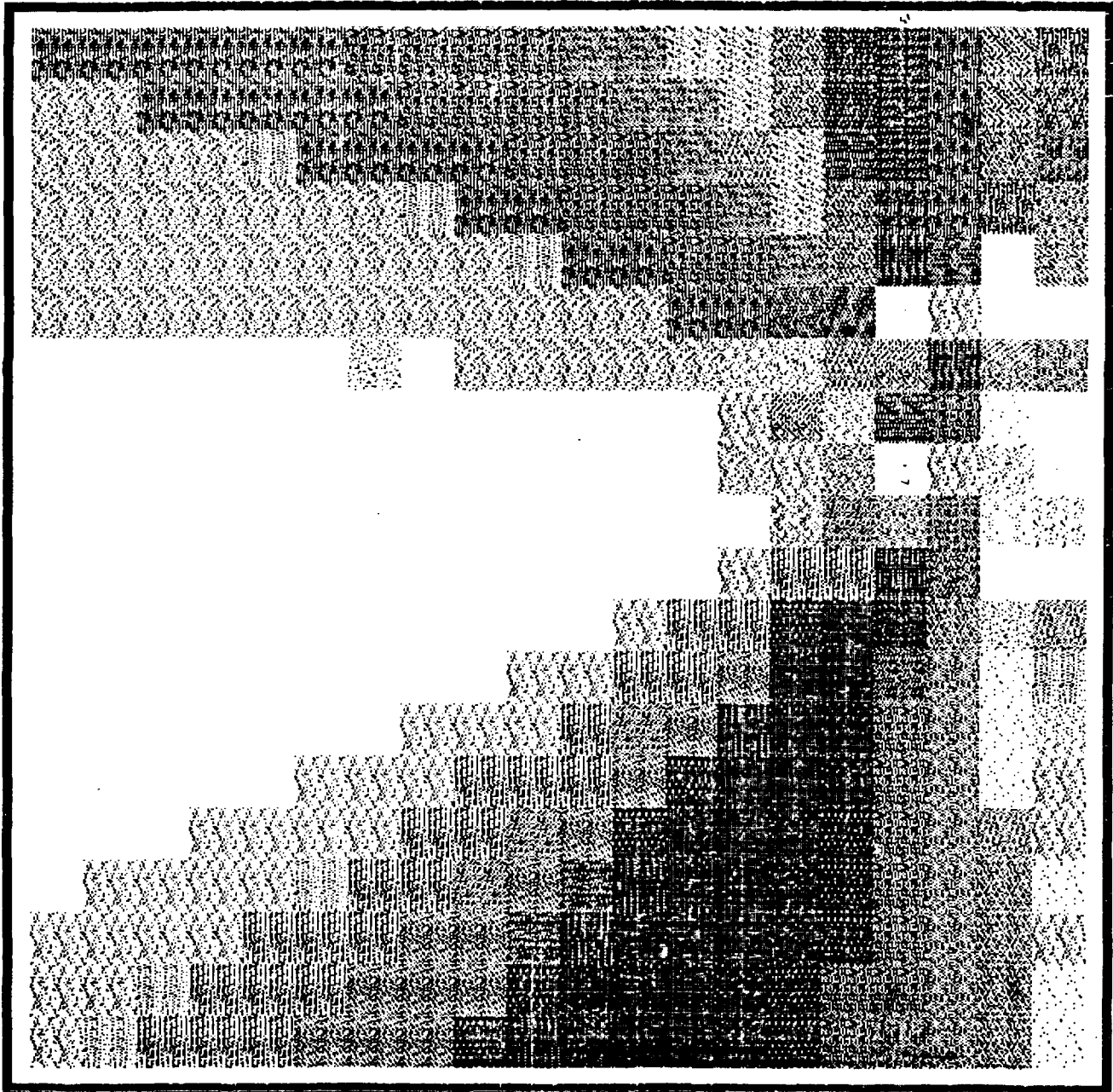
CHEVRON 3B - C, N, E (PIS-27)

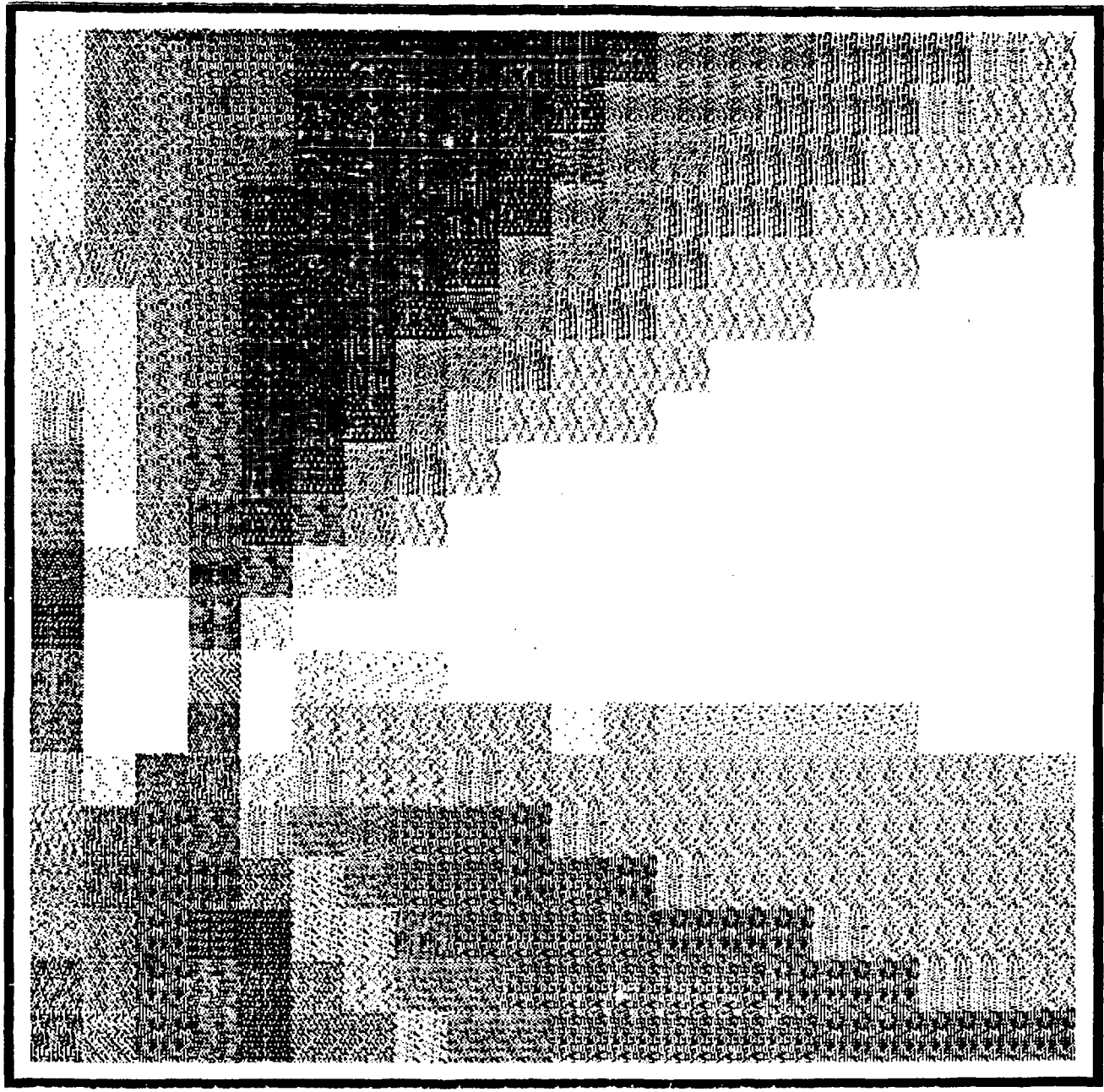
FOCUS (Product Version, Correlation Function reversed if negative) on  
 Filtered T.S., Pices 15-27 (Times 0725-0737), Mode 1,  
 CHEVRON Multi-Layer Vel. Prof. (See below),  
 XV Slices 1-4 (2000', 4000', 6000', 8000'), 20 \* 20 Grid

Density Plot of Same

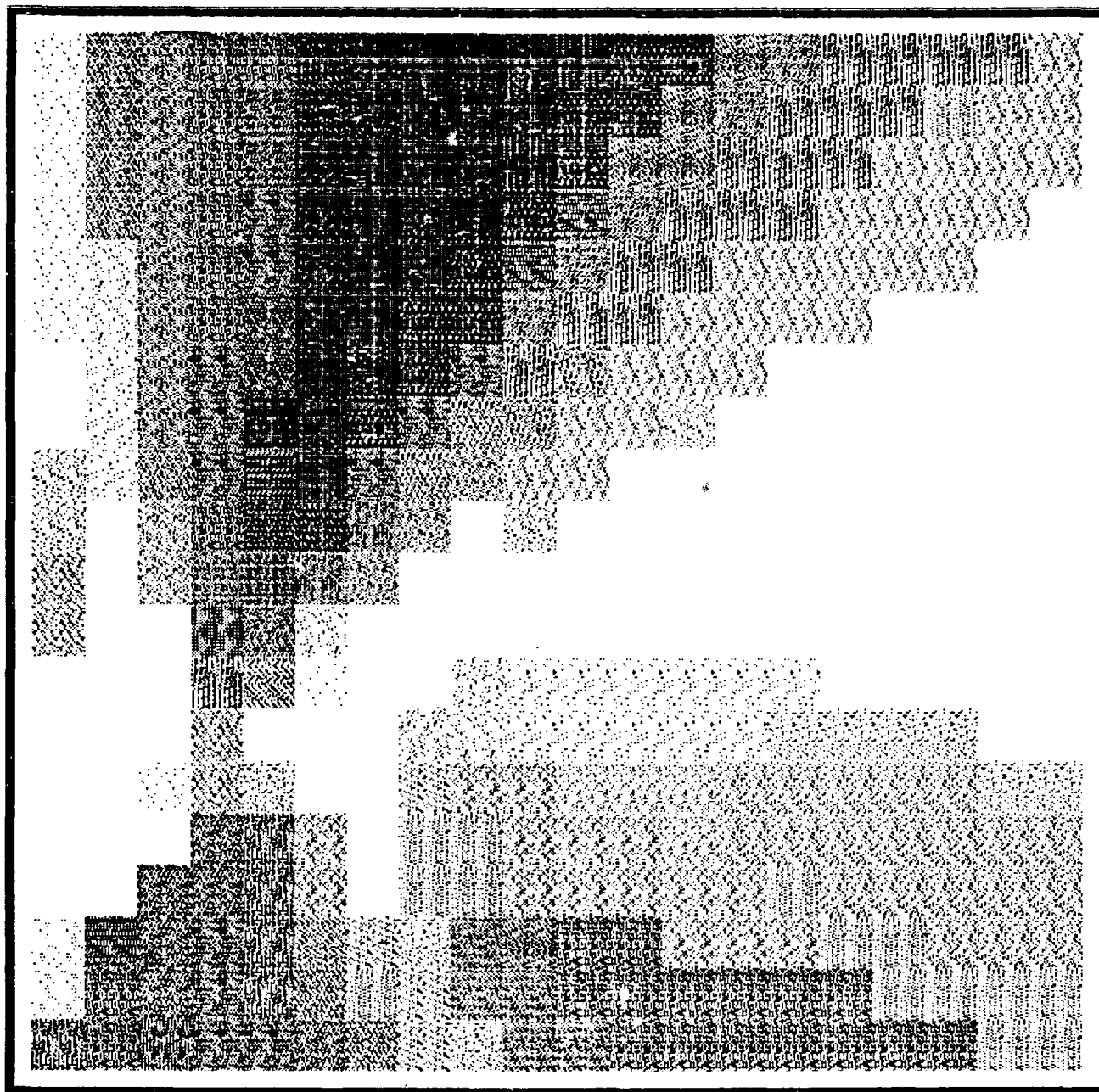
Layer #	Vel (ft/sec)	Layer (ft)
1	6000	0
2	7000	1600
3	8500	4600
4	9500	8200
5	11000	12200
6	12000	15500
7	14000	17000
8	16000	20000

Station 3



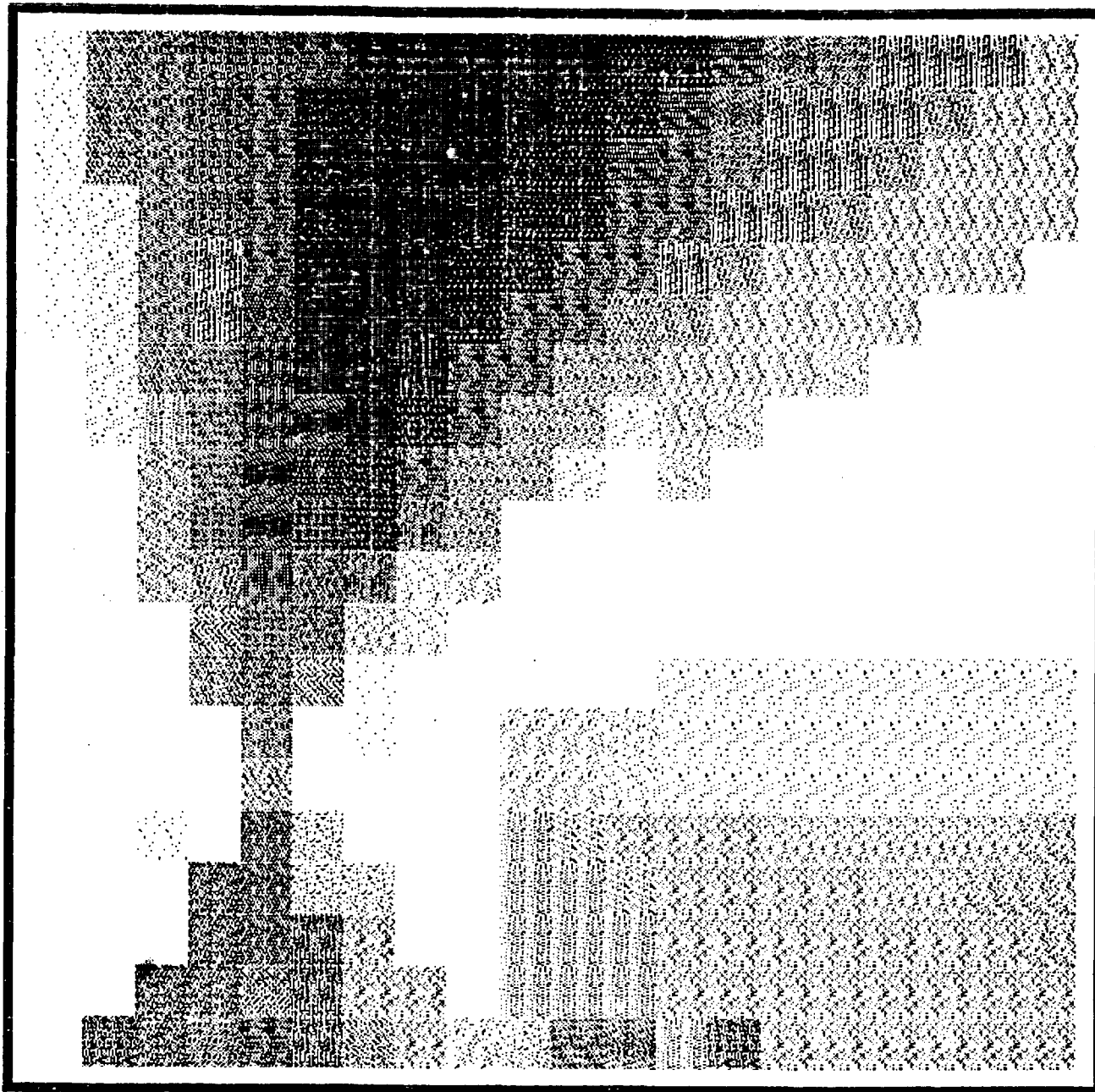


ENSCO, INC.



ENSCO, INC.





ENSCO, INC.

11/14, 7

Braun

ESS120 (Tand 4' 34")

COMP3D/DSP3D on CH4-CESW (P1-15)

INPUT: LUNA (97) BARC-1F31 (Print of FOC(305, Pnd 6) on  
CH4-CESW Filter: T.S., P. 15 (Times 0331, 0333-0346), Model 1,  
VF=1.0, NYR 10/28/77-1 (C1156), X/1-4 (rows,  
4000', 1000', 8000'), 20 x 20 Grid

DSP3D BARC-1F32 (Tand)

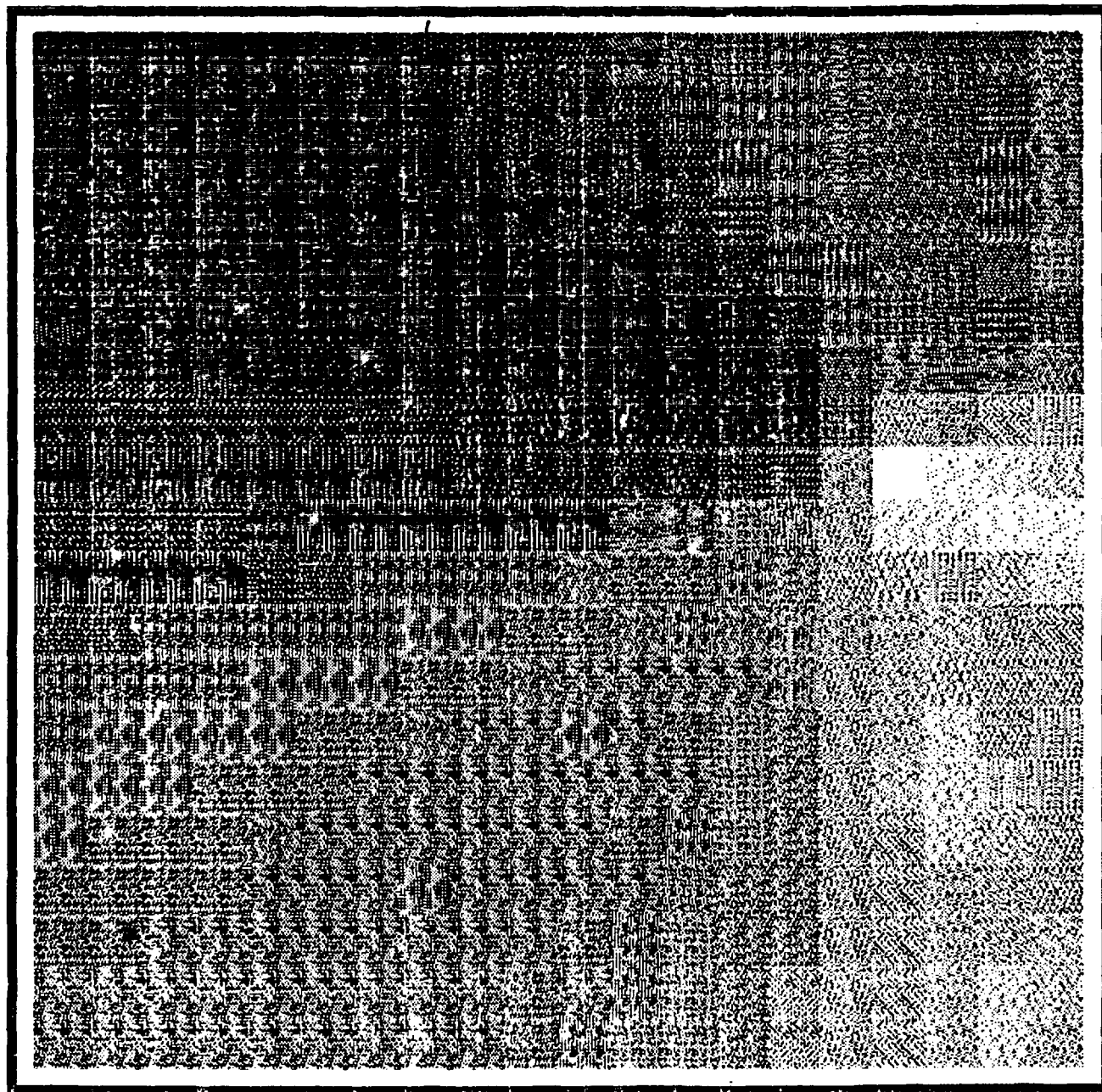
Copy 2 of 2  
CHEVRON 4-CESW (P1-15)

FOCUS (Product Version, Correlation Function (reversed if negative) on  
Filtered T.S., Pieces 1-15 (Times 0331, 0333-0346), Model 1,  
CHEVRON Single Layer Vel. Prof. (16000 ft/sec or 4.88 km/sec),  
XY Slices 1-4 (2000', 4000', 6000', 8000'), 20 x 20 Grid

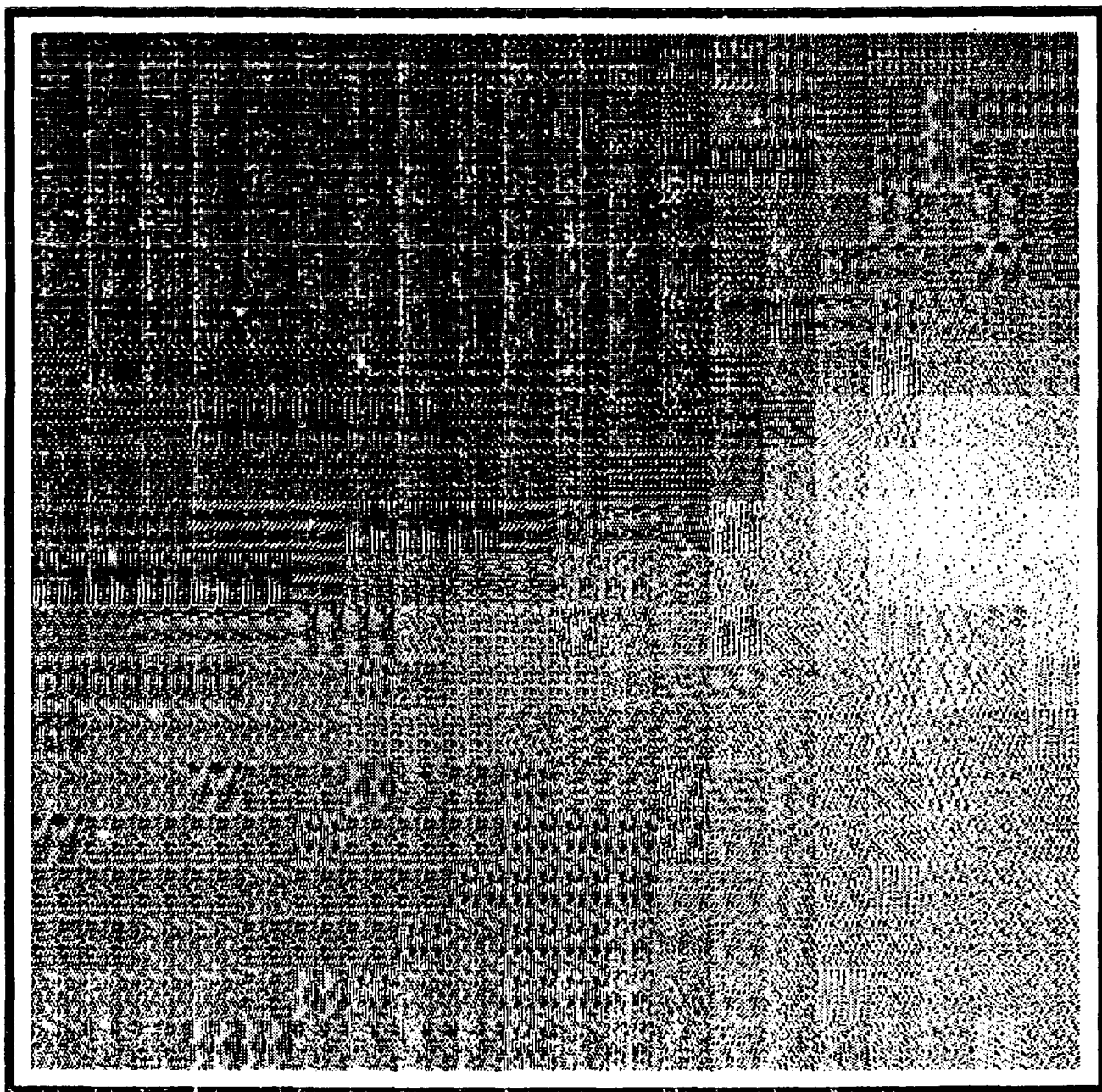
&

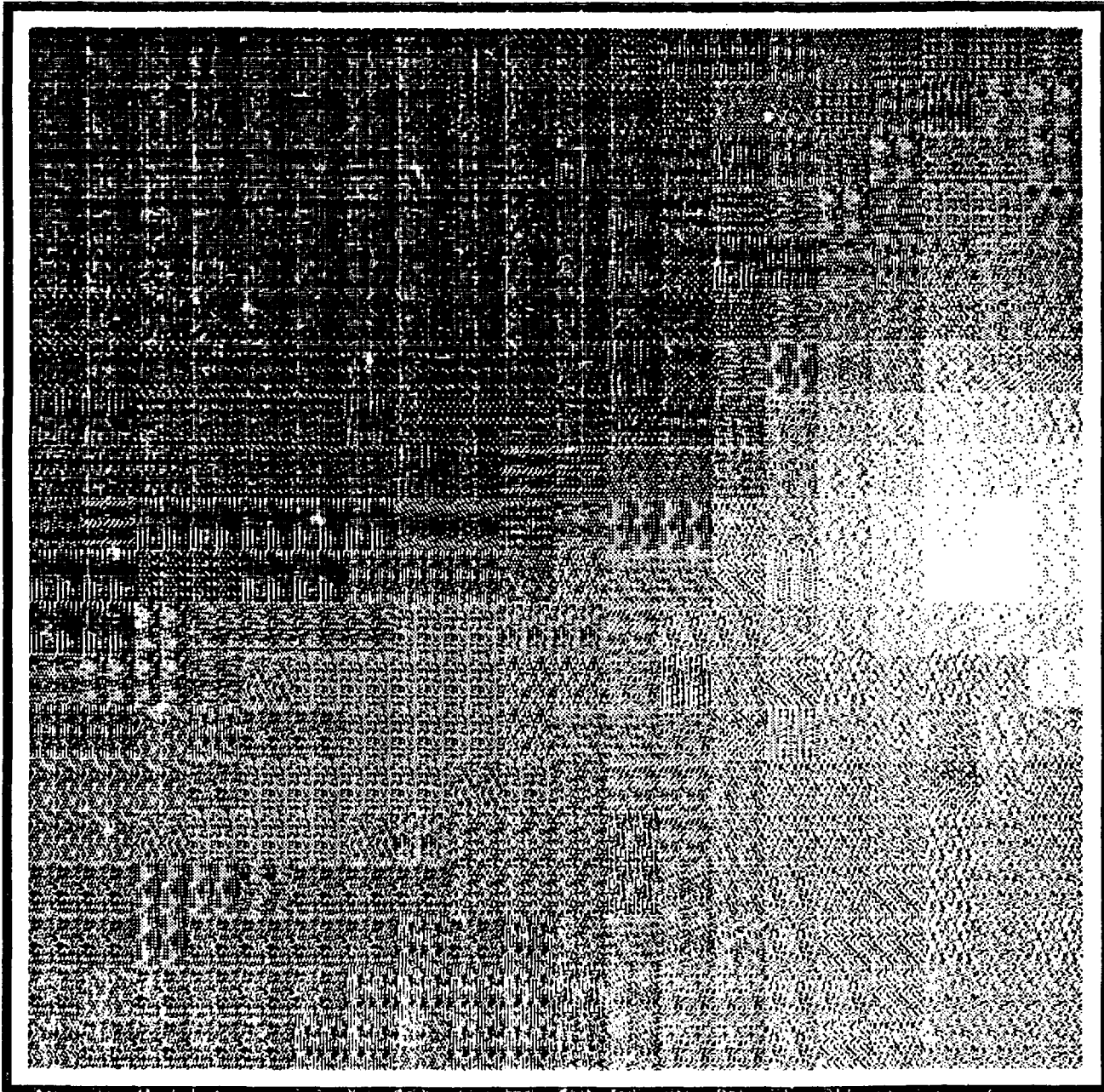
clonality Part of Same











11/10/77

Baumman

ESSW (Time 4'33")

"(CNOJO/DSPD)" in CHS-ESW (P1-15)

IMAG: LUNG (GT), BARC-1 Fv7 (Pnd HFOC<sub>30</sub> [Fvdc] in  
CHS-ESW filter. TS, P1-15 (T0936-50), Mode 1,  
VF=1.0, NYPO 10/28/77-01 (CHS), XY1-11/2000,  
4000, 6000, 8000', 20 x 20 grid

"(DISP)" BARC-1 Fv7 (Case 1)

Copy 2 of 2

CHEURON 5-ESW (P1-15)

Focus (Product Version, Correlation Function reversed if negative) on  
Filtered T.S., Pieces 1-15 (Time, 0936-0950), Mode 1,

CHEURON Single Layer Vel Profile (16000 ft/sec or 4.88 km/sec),

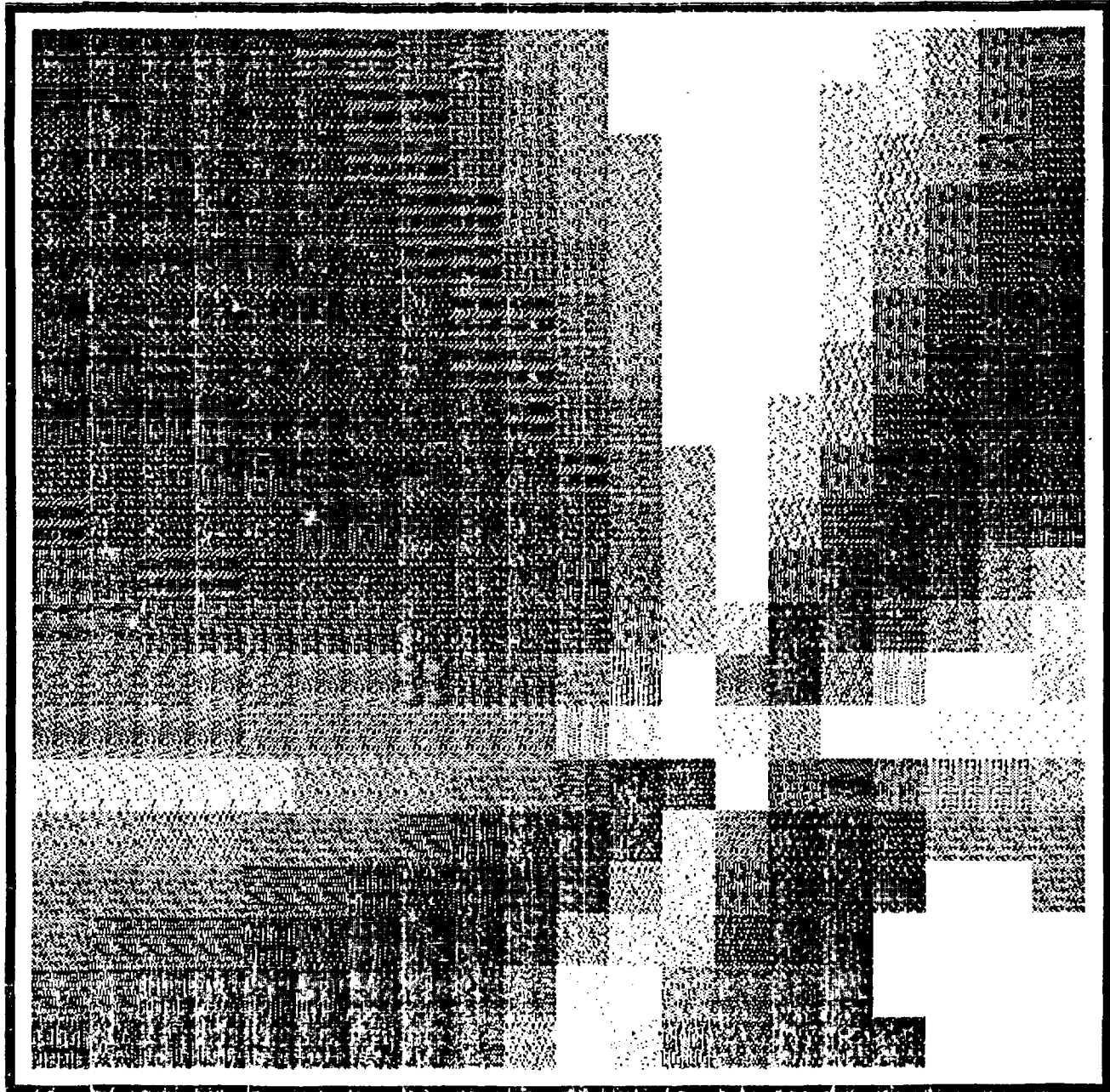
XY Slices 1-4 (2000', 4000', 6000', 8000'), 20 x 20 Grid

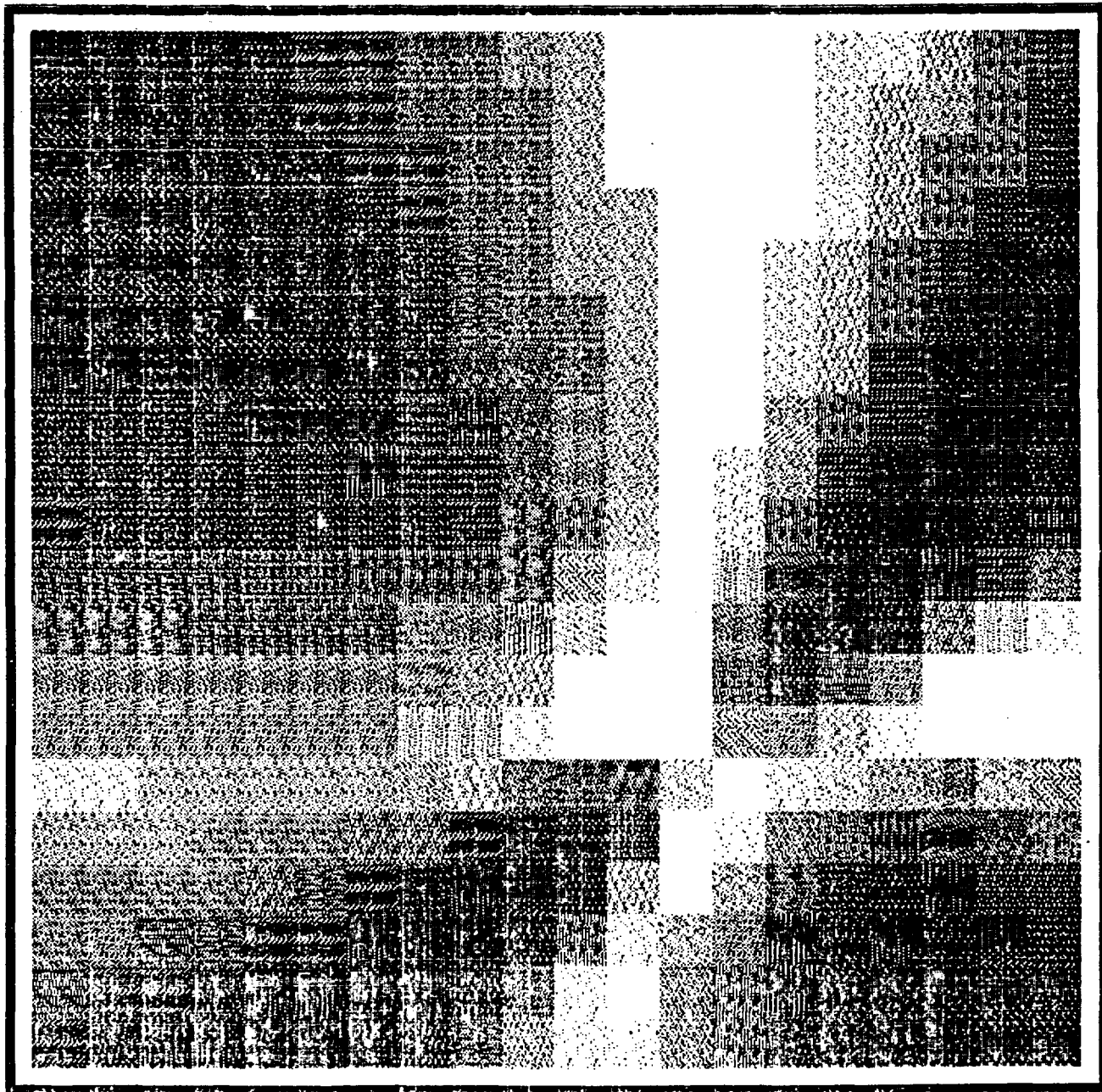
+

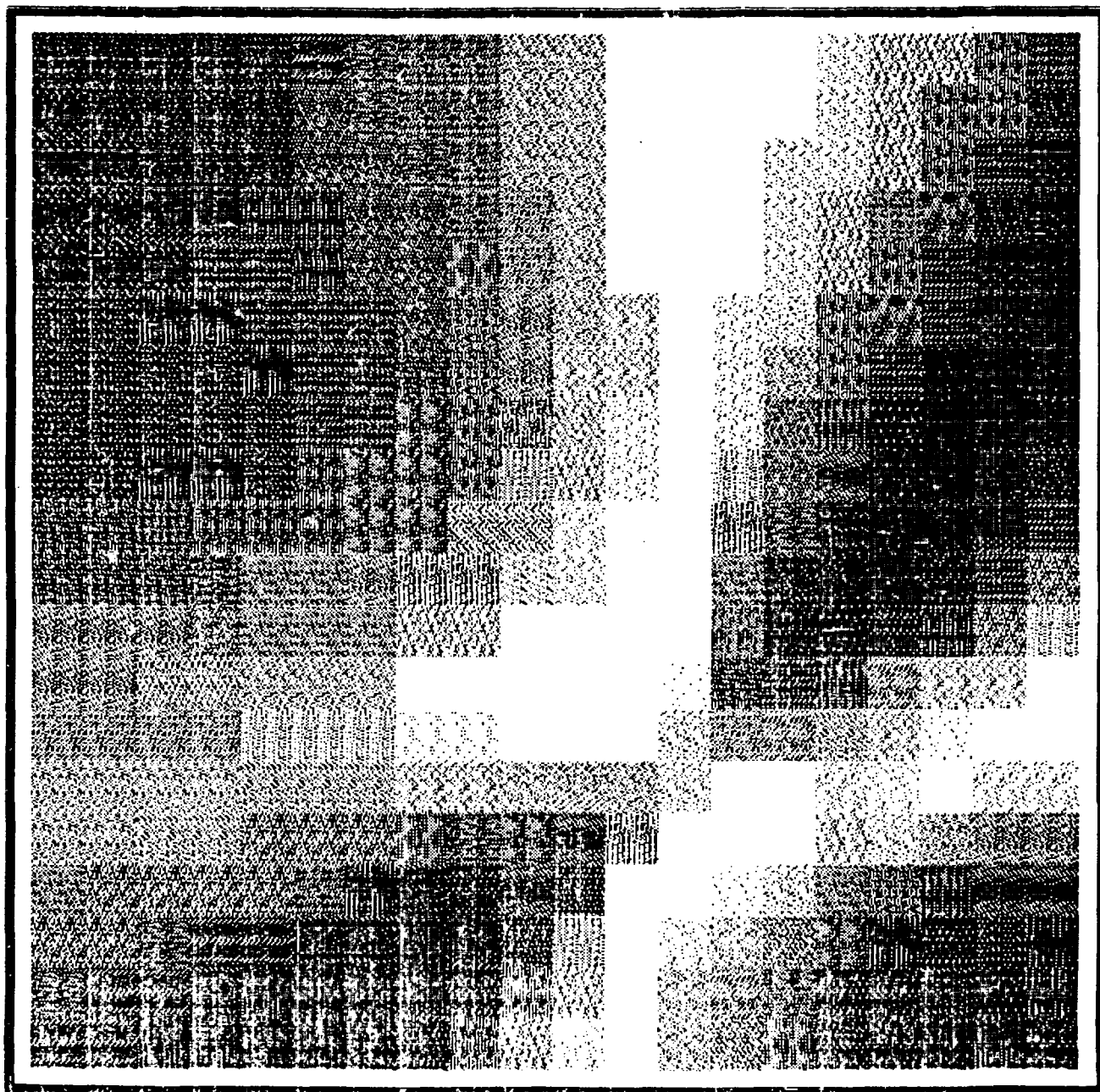
Assembly Plot of Same

Station 5

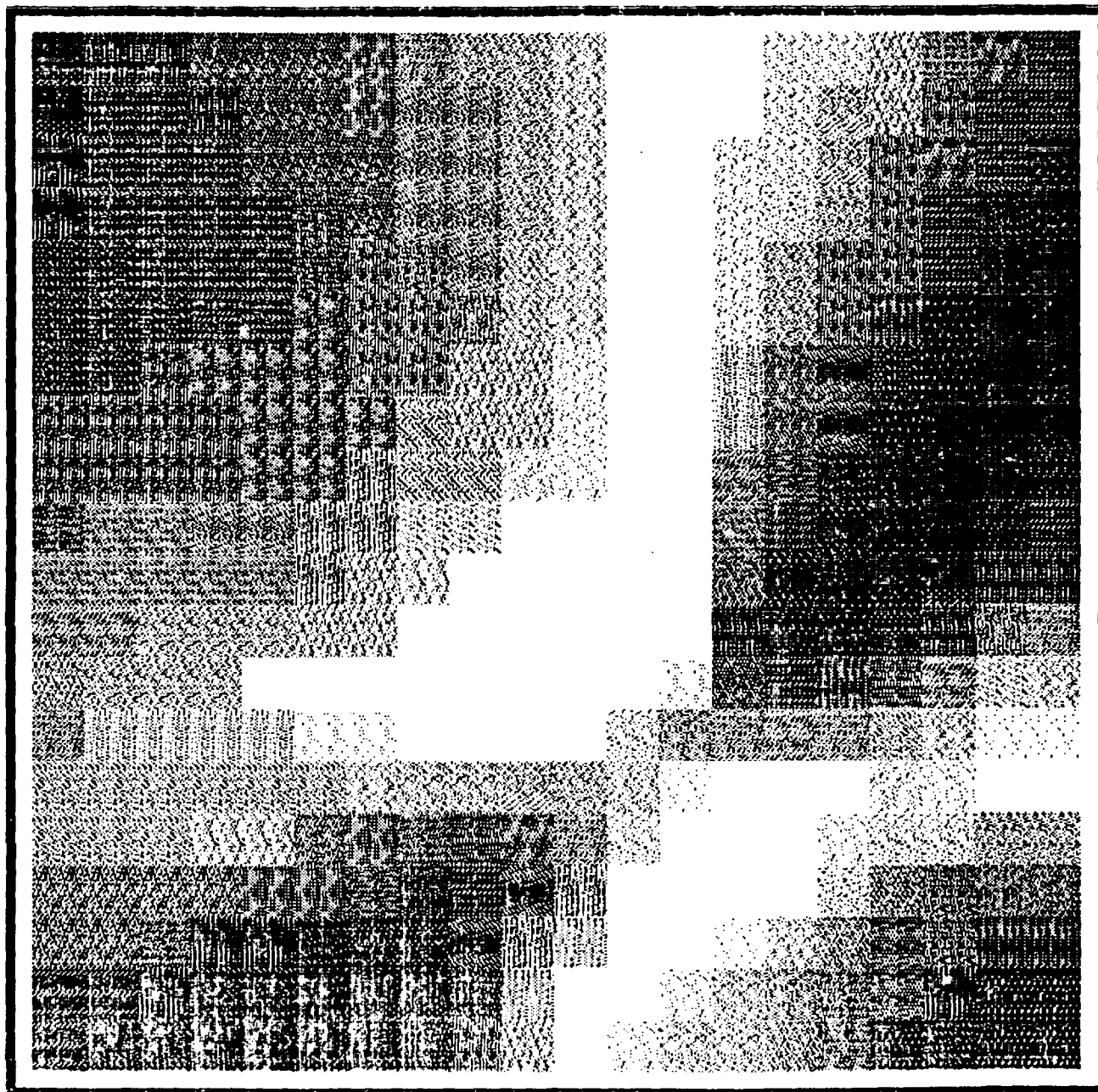












15:43 } 6:30  
 :DT  
 12/15/77 15:22:13  
 :IO, 8, 17, 10, L5, 9, 28, 7, 30  
 :RW, 8, 10  
 :QUB, DISP3D/ISR  
 0 0 1 4 0 0 0 0 0 0 0 0 0 0 0 0  
 20 20 0 0

FATER  
 580

12/15/77

Rauman

ESS1205 (Time 6'30")

-DISP3D on CH Controls (Max WT)

INSTR: LONG (GT.) RSTORC FI (3B-CNE  
 [PI-15 Filt], 5-ESW (PI-15 Filt), 1-MESW (PI-15 Filt)  
 4-CESW (PI-15 Filt)) WT. MAX

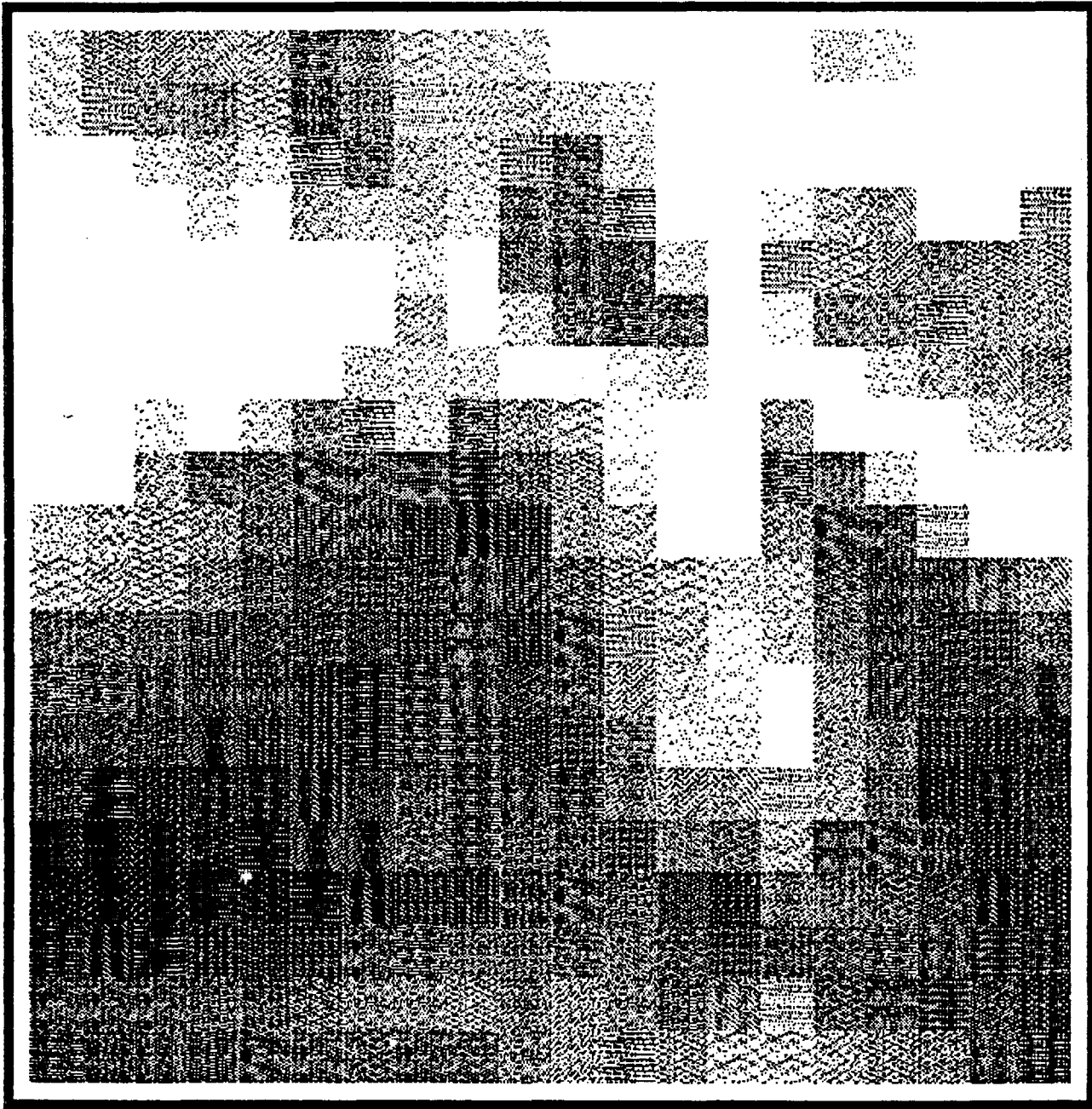
CHEVRON - COMPOSITE DENSITY PLOT (MATT.)

Composite of 3B-CNE (PI-15 Filt), 5-ESW (PI-15 Filt),  
 1-MESW (PI-15 Filt), 4-CESW (PI-15 Filt)

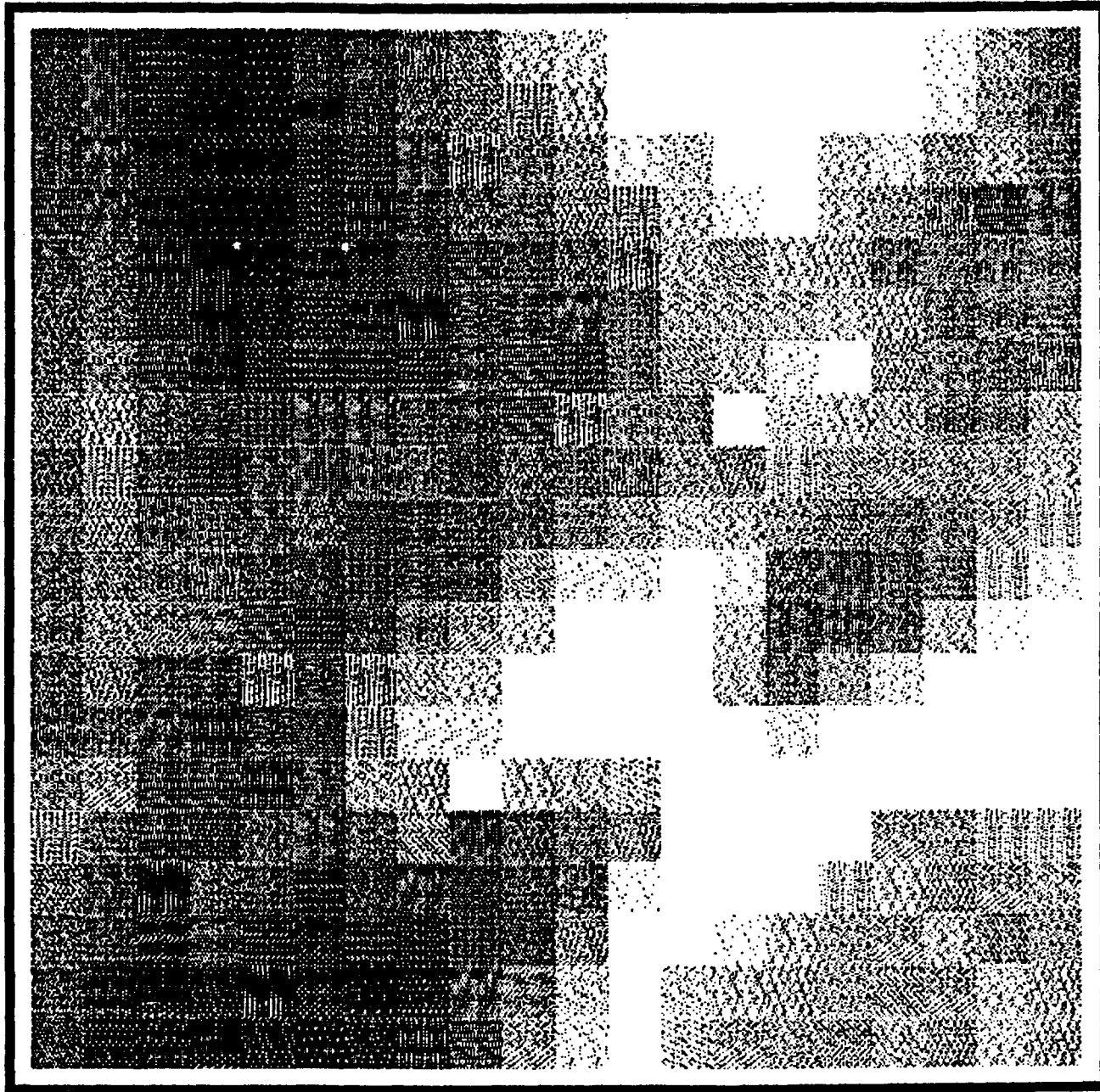
Remained 1/3 May background  
 Matt .3

Composite

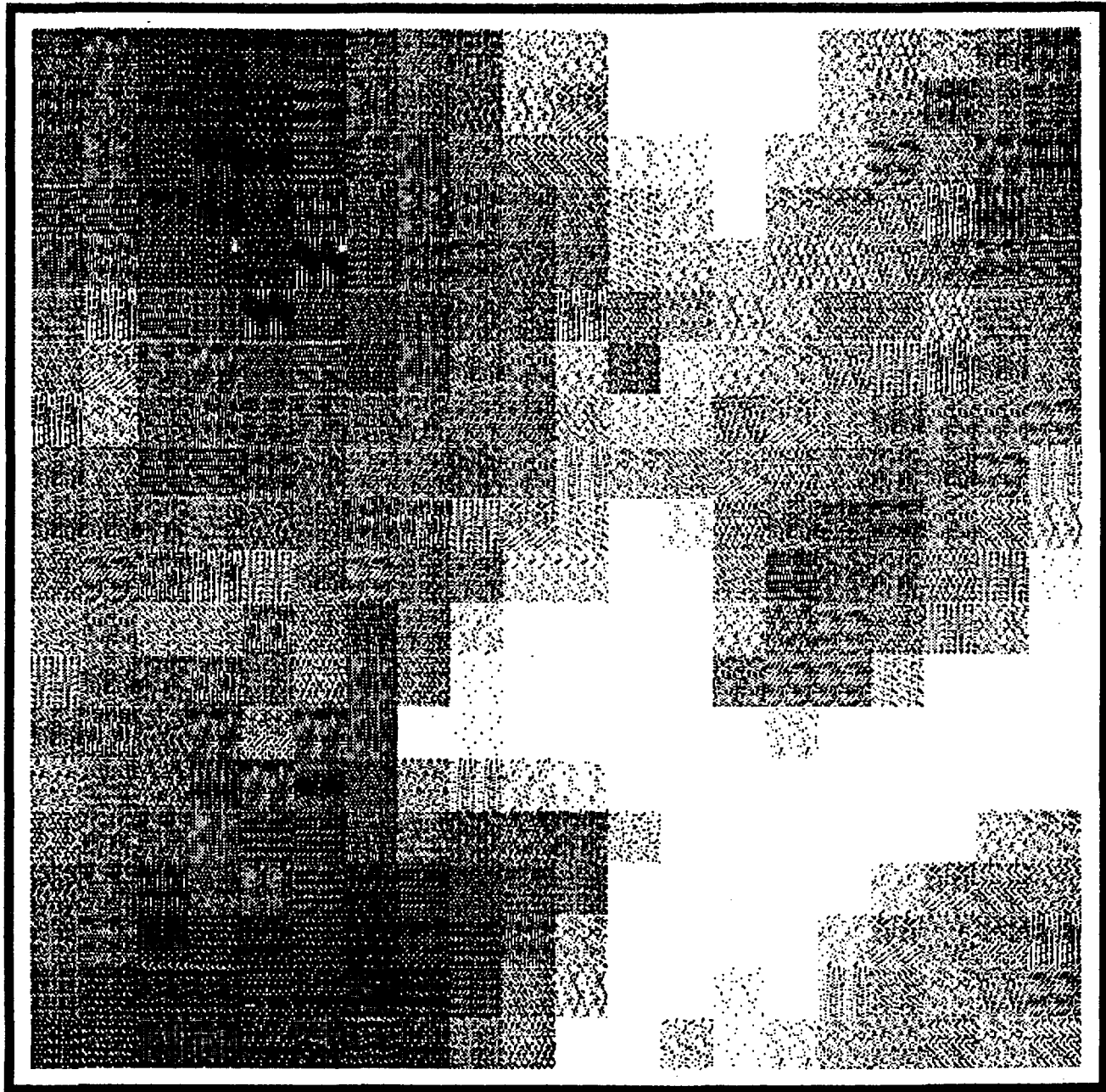
XY PLOT SLICE 1



ENSCO, INC.

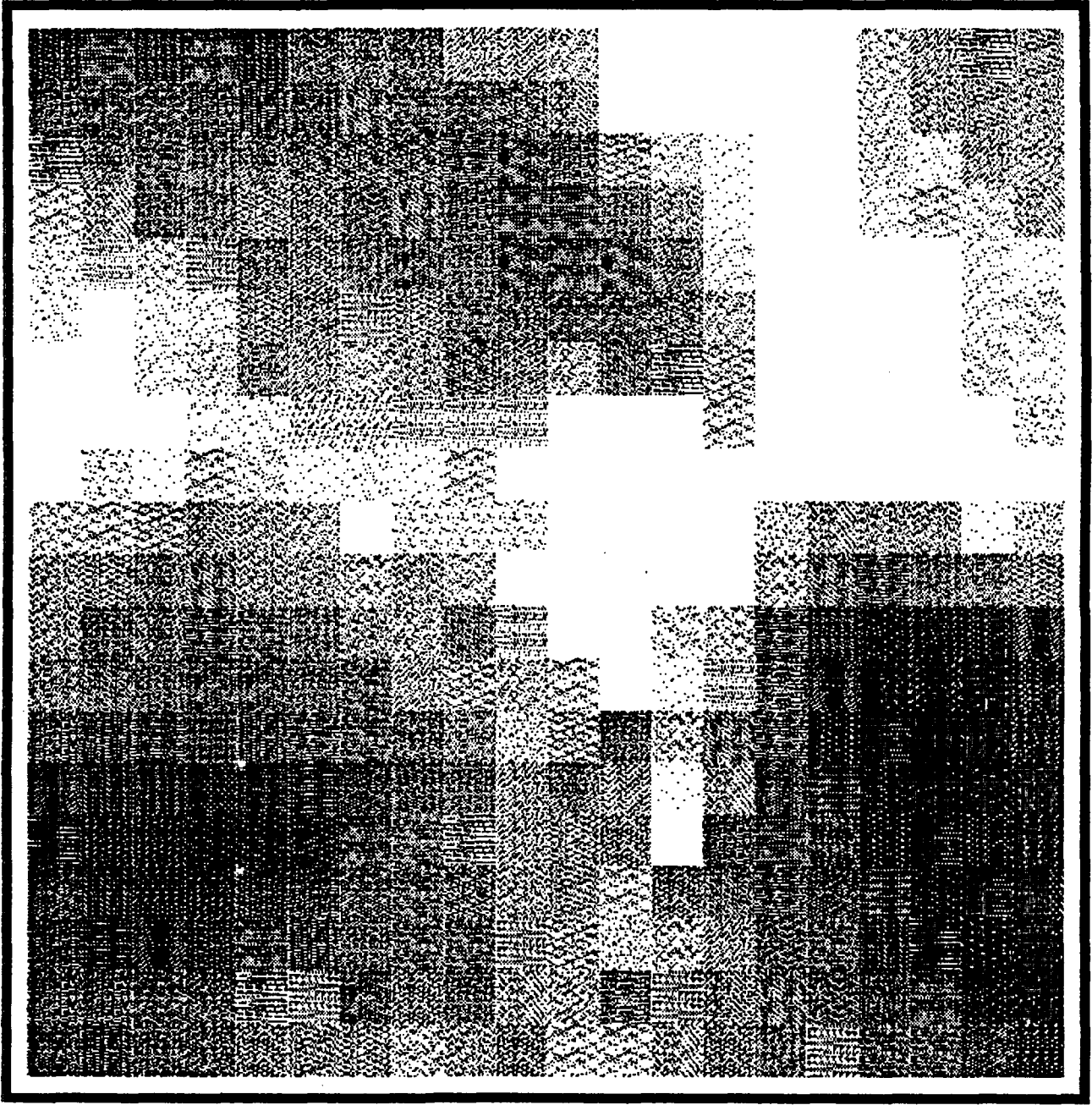


ENSCO, INC.



ENSCO, INC.

XY PLOT SLICE 4



ENSCO, INC.